Finite Element Modelling of Air-Coupled Circular Capacitive Micromachined Ultrasonic Transducer for Anodic Bonding Process using SOI Wafer

Gurpreet Singh Gill (er.gsgill@gmail.com)
University of Western Australia
Sanjay Kumar
IIT Indore: Indian Institute of Technology Indore
Ravindra Mukhiya (rmukhiya@ceeri.res.in)
Central Electronics Engineering Research Institute CSIR
Vinod Kumar Khanna
Central Electronics Engineering Research Institute CSIR

Research Article

Keywords: CMUT, FEM Modelling, Resonance Frequency, Pull-in

Posted Date: June 2nd, 2021

DOI: https://doi.org/10.21203/rs.3.rs-411793/v1

Abstract

Capacitive Micromachined Ultrasonic Transducer (CMUT) provides an alternative to commercial piezoelectric-based ultrasonic transducers due to its wide bandwidth, improved efficiency, sensitivity, and design flexibility [1, 2]. In this paper, Finite Element Method-based design and simulations of circular capacitive micromachined ultrasonic transducer (CMUT) is presented. The FEM simulation of air-coupled CMUT was accomplished by using MEMCAD tools CoventorWare® and COMSOL™. The resonance frequency of 3.9 MHz was achieved for the designed circular CMUT device. A favourable agreement was found for the resonance frequency and pull-in voltage of the device using MEMSCAD tools and analytical calculations. For the proposed CMUT design, a circular cavity will be formed inside the glass substrate. Then, a free-standing membrane will be released using active layer of silicon-on-insulator (SOI) wafer. The bulk silicon of SOI wafer will be removed after bonding it on the glass substrate using anodic bonding technique as described in fabrication process flow for CMUT.

1. Introduction

Ultrasonic waves ranging from 2–18 MHz are commonly used for curative applications, and generated by ultrasonic transducers [3]. Nowadays, Micro-Electro-Mechanical System (MEMS) based Capacitive Micromachined Ultrasonic Transducers are used for this purpose. The piezoelectric transducers have been used for medical imaging applications during the last 50 years. However, due to impedance mismatching with air, self-heating, high dielectric losses at high frequencies and austere geometric tolerances in the piezoelectric transducers, the technology has taken a stride towards the capacitive transducers [4–9] for therapeutic applications. The basic principle of operation is based on the thin film vibrations, when subjected to an electrostatic force for generating and sensing sonic waves [8]. The vacuum-sealed and unsealed devices were developed for this operation, ranging in radius from a few microns to several hundred microns [4, 8]. CMUTs are generally fabricated using sacrificial release method and wafer bonding technique. In the case of standard sacrificial release method, the membrane is released by using MEMS surface micromaching techniques. While, bonding techniques for instance anodic bonding, fusion bonding and adhesive bonding are generally used for the fabrication of pressure sensors and accelerometers. For achieving high membrane uniformity the wafer-bonding technique is highly recommended, although, it is a bulky process [10].

This paper summarizes the comparative study of analytical and simulation results for the circular CMUT device to be realized by the anodic wafer bonding technique using SOI wafer. The operation modes and device description of CMUT are presented in the Sect. 2. In the Sect. 3, the mathematical analysis is discussed. The simulation study is revealed in the Sect. 4. Moreover, the results and discussion part is delineated in Sect. 5. A complete fabrication flow for CMUT is explained in Sect. 6. Finally, conclusions are drawn in the Sect. 7.

2. Device Description

The capacitive micromachined ultrasonic transducers are used for generating ultrasound frequencies in the range of several Mega-Hertz. The working principle is based on the “electrostatic” phenomena. Normally, the capacitive micromachined ultrasonic transducers are operated in two modes: transmitter mode and receiver mode. In the transmitter mode, DC voltage is applied between top and bottom electrodes. Due to applied DC potential, the electrostatic force is generated and membrane deflects towards the bottom electrode. After that, an AC signal of frequency, which is equivalent to first mode of natural frequency of the membrane, is superimposed on the DC voltage. Ultrasonic waves are generated with respect to applied AC signal frequency. In the receiver mode, the ultrasonic waves impinge on the membrane and correspondingly the membrane is deflected. In this case, the applied DC potential is fixed and membrane vibrates due to applied ultrasonic waves [8]. Furthermore, CMUTs also have two other modes known as collapsed mode (pull-in) and non-collapsed mode. In the case of collapsed mode, membrane is physically connected to the bottom electrode or substrate surface. While, in the case of non-collapsed mode, the membrane does not have any physical contact with the bottom electrode.

The representation of proposed capacitive micromachined ultrasound transducer is revealed in Fig. 1. In this structure, the bottom electrode is fixed on the glass (Pyrex) substrate and top electrode is mounted on the suspended membrane. The resonance frequency of CMUT is dependent on the material properties, membrane thickness, membrane diameter and shape of membrane. Table 1 shows the device dimensions and parameters. Typically, a CMUT has parallel-plate capacitor structure, the first metal electrode is fixed on the glass substrate known as bottom electrode, and the second metal electrode is placed on movable membrane known as top electrode. The 0.3 μm cavity is formed between the top and bottom electrodes. The membrane is formed by using the silicon-on-insulator (SOI) wafer. The cavity is created inside the Pyrex glass [11, 12]. The physical parameters of CMUT device have been designed using FEM-based MEMSCAD tools for a frequency of 3.9 MHz for therapy applications.

Table 1
Design shape, parameters and dimensions for all the layers selected for the analytical and simulation study of CMUT.

Parameter	Dimension
Base material	Silicon and Pyrex
Membrane material	Silicon and Silicon dioxide
Shape of the membrane	Circular
Size of the membrane	90 μm (Diameter)
Thickness of the membrane	2 μm Si and 1 μm SiO_2
Air cavity height	0.3 μm
Top/bottom electrode	Ti/Cr + Gold
Electrode thickness	220 nm

3. Mathematical Analysis

For the CMUT device, we started the design with the analytical modelling of the device and then FEM simulations were performed. The resonance frequency response of the CMUT device depend upon the device parameters and material properties. The resonance frequency is calculated by formula given in Eq. 1, and is found to be 4.1 MHz [14].

$$f_r = \frac{0.47h}{a^2}\sqrt{\frac{E}{\rho(1-\nu^2)}}$$

1

.....

where, a is the radius of the membrane, h is the thickness of the membrane, E is the Young's modulus, ν is the Poisson's ratio and ρ is the density of the material. It is clear from this formula that the response of resonance

for a CMUT device is directly proportional to the thickness of the membrane and Young's modulus of the material. However, it is inversely proportional to the radius of the membrane, Poisson's ratio, and density of the material.

For the transmission mode operation of the device, the DC voltage is applied between two electrodes, which leads to the generation of electrostatic force between the plates of the device defined by Eq. 2.

$$F_{electrostatic} = \left[\frac{\pi a^2}{2\left(d_0 - w\right)^2} + \frac{a}{\left(d_0 - w\right)} - 1.918\right]\epsilon_0 V^2$$

2

where, d_0 is the gap between membrane and bottom electrode, w is the distance travelled by membrane, ε_0 is the dielectric permittivity of free space, and V is the applied DC voltage. Due to the electrostatic force, the electrostatic pressure is also induced and is expressed by the following equation, Eq. 3 [15].

$$P_{electrostatic} = \epsilon_0 V^2\left[\frac{1}{2d_0^2} + \frac{1}{\pi a d_0} - \frac{1.918}{\pi a^2}\right] - \epsilon_0 V^2\left[\frac{1}{d_0^3} + \frac{1}{\pi a d_0^2}\right]w_0$$

3

To compensate for the effect of electrostatic pressure, a reverse pressure known as elastic restoring pressure is also generated inside the membrane in the direction opposite to the electrostatic pressure; it is

$$P_{elastic} = \left[\frac{4\sigma h}{a^2} + \frac{64D}{a^4}\right]w_0 + \left[\frac{128\alpha D}{h^2 a^4}\right]w_0^3$$

4

where, $D = \frac{\tilde{E}h^3}{12(1-\nu^2)}$ is the flexural rigidity, $\tilde{E} = \frac{E}{1-\nu^2}$ is the effective young's modulus, $\alpha = \frac{7505+4250\nu-2791\nu^2}{35280}$ is an empirical parameter depending on Poisson's ratio, and σ is the residual stress. In equation (4), the first term

denotes the combined stiffness due to bending and residual stress, and second term defines the stiffness of the membrane due to non-linear stretching.

For the parallel plate actuator, distance travelled by diaphragm (membrane) for pull-in to occur is equal to one third of the total gap between the two plates of the actuator

$$w_{0-PI} = \frac{d_0}{3}$$

5

By substituting Eq. (5) in Eq. (3) and Eq. (4), we got the following two important equations:

$$P_{PI-electrostatic} = \epsilon_0 V^2 \left[\frac{1}{2d_0^2} + \frac{1}{\pi a d_0} - \frac{1.918}{\pi a^2}\right] - \epsilon_0 V^2 \left[\frac{1}{d_0^3} + \frac{1}{\pi a d_0^2}\right]\left[\frac{d_0}{3}\right]$$

6

$$P_{PI-elastic} = \left[\frac{4\sigma h}{a^2} + \frac{64D}{a^4}\right]\left[\frac{d_0}{3}\right] + \left[\frac{128\alpha D}{h^2 a^4}\right]\left[\frac{d_0}{3}\right]^3$$

7

By using the above two equations (6) and (7), we calculate the pull-in voltage for the membrane. The pull-in voltage is defined as the voltage value at which the membrane collapses at bottom electrode. The collapse voltage determined by Eq. (8) is 80.09 V.

$$V_{PI} = \sqrt{\frac{\left[\frac{64D}{a^4} + \frac{4\sigma h}{a^2}\right]\left(\frac{d_0}{3}\right) + \frac{128\alpha D}{h^2 a^4}\left(\frac{d_0}{3}\right)^3}{\epsilon_0\left[\frac{1}{6d_0^2} + \frac{2}{3\pi a d_0} - \frac{1.918}{\pi a^2}\right]}}$$

8

4. Fem Simulations

The simulation of CMUT has been performed using MEMCAD tools CoventorWare® and COMSOL™. The MemMech module of CoventorWare® has been used for modal analysis and for harmonic analysis the HarmonicEM module has been used. Figures 2 and 3 show the process flow used to create a three-dimensional (3-D) model and cross-sectional view of CMUT device using CoventorWare® and COMSOL™, respectively. The materials and their properties used during the simulation process are given in the Table 2. In the whole process, the surface boundary condition has been set to “fixed all direction” [12, 13]. In the case of COMSOL™, the Electromechanics interface is used to compute solid mechanics and electrostatics with a moving mesh collaboratively to model the deformation of electrostatically actuated structures. The displacement, stress and strain are computed using Solid Mechanics interface, while the Electrostatics interface is used to compute the electric field, electric displacement field and potential distributions in dielectrics under conditions where the electric charge distribution is explicitly prescribed. It is very easy to combine two or more physics in this tool such as eigenfrequency, frequency-domain, small-signal analysis, and time-domain modeling because of it’s stationary formulation and are supported in all space dimensions.

Table 2
Materials properties such as young’s modulus, poison’s ratio, and density used in the simulation for silicon, silicon dioxide, and gold.

Materials	Young’s Modulus E (GPa)	Poison’s Ratio (v)	Density ρ (kg/m^3)
Silicon	169	0.27	2300
Silicon dioxide	70	0.17	2200
Gold	57	0.35	19300

The DC boundary condition has been applied as 65 V to the top electrode and bottom electrode set to 0 V. AC boundary condition of 6.5 V has been superimposed on DC to the top electrode. For the MemMech analysis, the same boundary condition and material property with residual stress has been used [6–8]. The outer boundary of suspended membrane and substrate are set to be fixed under MemMech BCs. For the damping analysis, the DampingMM module has been used. For this purpose, tetrahedron meshing is used in all the studies. The following section shows all the results of circular CMUT. In the case of

al boundary and all the side faces are fixed; only

z-direction movement is allowed. Moreover, free tetrahedral meshing is implemented to find eigenfrequency, change in frequency, change in capacitance, and maximum displacement on applying DC voltage.

5. Results And Discussion

Figure 4 shows the simulation results obtained using CoventorWare®. Figure 4(a) shows the modal analysis result, in which the natural frequency of CMUT device is found to be 3.9 MHz. The maximum displacement, 9.9×10^{-5} μm, and phase shift of 90 degree are achieved at a resonance frequency of 3.9MHz, on applying AC with DC voltages to the electrodes, while performing the harmonic analysis using CoSolveEM Settings, is shown in the Figs. 4(b) and 4(c), respectively. With the electrostatic force, the membrane attains the maximum displacement at the resonance frequency. In conventional mode, the maximum deflection is accomplished by the membrane before the collapse. Figure 4(d) shows the relation between velocity and frequency, in which, when AC signal is superimposed along with DC voltage then the membrane starts to vibrate at the resonance frequency. Hence, the membrane velocity of 1.65×10^{-11} μm/s is depicted at the resonance frequency. The correlation between dissipation energy and frequency is represented in the Fig. 4(e). Owing to energy conversion law, when any mechanical part of device is moving from one position to another, a small amount of energy is generated and dissipates in the form of heat. Therefore, 2.25×10^{-33} μNm energy is dissipated from membrane on vibrations at resonance frequency. Figures 4(f) and (g) indicate that the value of damping coefficient is 2.39×10^{-7} N/(m/s), damping force is 5.93N/m, and spring force is 393.68 N/m at resonance frequency, when subjected to DampingMM analysis at the atmospheric pressure. Under the effect of electrostatic force, a restoring force is generated inside the device known as spring force. The spring force has gradually increased with frequency and at the certain value of frequency it gets saturated. In Fig. 4(h) for the transient analysis, a time depending study is performed. In this case, a 65 V DC signal is applied on the top electrode and bottom electrode is kept grounded. It is observed that time required to reach the steady state position for the membrane is 2.5 μs.

After performing the analysis using CoventorWare® simulation tool more analysis, for instance biased eigenfrequency, change in frequency and change in capacitance with respect to applied DC voltage are computed using COMSOL™, MEMSCAD tool portrayed in the Fig. 5. Figure 5(a) describes the unbiased mode Eigen frequency, 3.91 MHz. It is clear from Fig. 5(b) that the resonance frequency of the CMUT device decreases with increase in the DC voltage owing to spring softening effect. However, the capacitance value between top and bottom electrode increases with increasing value of applied voltage (see Fig 5(d)) because of decrease of the distance between the electrodes. Moreover, the displacement of the membrane on applying the DC voltage is presented in the Figs. 5 (c) and (e). It is also clear from the graphs that the condition for pull-in, , is satisfied at 73 V. An abrupt downfall is noticed in the membrane deflection, and finally, it touches the substrate and starts operating in collapsed mode. In addition to that, the resonance frequency response of 4.1 MHz and pull-in voltage of 80.09 V are also calculated

6. Fabrication Process Flow

The fabrication process flow of complete CMUT device is shown in Fig. 6. The steps involved in fabrication of free standing CMUT membrane are as follow:

I. First of all a glass wafer will be selected for the fabrication. The patterning of the glass wafer will be performed by spinning photoresist on it in order to etch air cavity inside the glass as shown in Fig. 6(a).

II. The etching of glass will be performed with the help of buffered oxide solution, and the same photoresist mask is used for the deposition of bottom gold electrode, as depicted in Fig. 6 (b), using sputtering technique. Figure 6 (c) shows the etched glass substrate with bottom gold electrode after the removal of unwanted gold with the help of acetone using lift-off process.

III. Now SOI wafer with 1 μm thick oxide layer and 2 μm thick device layer will be chosen for the anodic bonding process shown in Fig. 6 (d). Figure 6 (e) depicts the anodic bonded SOI wafer with the glass substrate.

IV. The bulk micromachining of handling silicon will be performed using an optimised Tetramethylammonium hydroxide (TMAH) process. For this a 25% TMAH solution will be used in order to suspend the device layer over the glass substrate. However, the bulk micromachining of the silicon can be done either by dry [12, 13] or wet micromaching technique [14, 15, 16]. These suspended membrane will be patterned again using photoresist to deposit top electrode using sputtering technique as illustrated in Fig. 6 (f). Finally, the unwanted golf is removed using lift of process in acetone solution as shown in Fig. 6 (g).

7. Conclusions

The simulation study of CMUT device has been successfully accomplished using MEMSCAD tools, CoventorWare® and COMSOL™. A favourable agreement between resonance frequency values of 3.91 MHz, 3.91 MHz and 4.1 MHz has been achieved using CoventorWare®, COMSOL™ and Analytical calculations, respectively. Similarly, the collapse voltages, 73 V and 80.09 V have been obtained using COMSOL™ and analytical calculations. The effect of DC voltage on membrane, resonance frequency, capacitance and displacement are also studied. It is concluded that for the maximum efficiency in the conventional mode, the applied voltage must be below the pull-in voltage, 73V but it should also be close to it. Finally, a fabrication method to fabricate the CMUT devices has been proposed.

Declarations

ACKNOWLEDGMENTS

The authors would like to express their sincere gratitude to Director, CSIR-CEERI, Pilani for his encouragement. They wish to thank all member of Smart Sensors Group at CEERI, and Vinod Kumar

Khanna is thankful to CSIR for grant under emeritus scientist scheme.

References

1. Jeong, B.G., Kim, D.K., Hong, S.W., Chung, S.W., Shin, H.J.: Performance and reliability of new CMUT design with improved efficiency. Sensors and Actuators A **199**, 325–333 (2013)
2. Song, J., Xue, C., He, C., Zhang, R., Mu, L., Cui, J., Miao, J., Liu, Y., Zhang, W.: “Capacitive Micromachined Ultrasonic Transducers (CMUTs)for Underwater Imaging Applications,” Sensors 2015, Vol. 15, pp. 23205–23217
3. Carovac, A., Smajlovic, F., Junuzovic, D.: Application of Ultrasound in Medicine. AIM **19**(3), 168–171 (2011)
4. Jin, X., Ladabaum, I., Khuri-Yakub, B.T.: The Microfabrication of Capacitive Ultrasonic Transducers. J. Microelectromech. Syst. **7**(3), 295–302 (1998)
5. Ladabaum, I., Khuri-Yakub, B.T., Spoliansky, D.: "Micromachined ultrasonic transducer: 11.4 MHz transmission in air and more". Applied Physics Letter **68**(1), 7–9 (1995)
6. Soh, H.T., Ladabaum, I., Atalar, A., Quate, C.F.: B. T. Khuri-Yakub, "Silicon micromachined ultrasonic immersion transducer". Applied Physics Letter **69**(24), 3674–3676 (1996)
7. Arora, A., Gopal, R., Dwivedi, V.K., Shekhar, C., Ahmad, B., Pratap, R., George, P.J.: "Fabricating Capacitive Micromachined Ultrasonic Transducers with Wafer Bonding Technique," Sensor & Transducers Journal, 93, 6, June 2008, 15–20
8. Ergun, A.S., Yaralioglu, G.G., Khuri-Yakub, B.T.: Capacitive Micromachined Ultrasonic Transducers: Theory and Technology. Journal of Aerospace Engineering **16**(2), 76–84 (April 2003)
9. Joseph, J., Singh, S.G., Vanjari, S.R.K., "Fabrication of SU-8 Based Capacitive Micromachined Ultrasonic Transducer for Low Frequency Therapeutic Applications," IEEE, 2015, pp. 1365–1368
10. Ergun, A.S., Huang, Y., Zhuang, X., Oralkan, O., Yaralioglu, G.G., Khuri-Yakub, B.T.: Capacitive Micromachined Ultrasonic Transducers: Fabrication Technology. IEEE Transactions on Ultrasonics, Ferroelectrics, And Frequency Control **52**(12), 2242–2258 (December 2005)
11. Park, K.K., Khuri-Yakub, B.T., et al., “Fabrication of Capacitive Micromachined Ultrasonic Transducers via Local Oxidation and Direct Wafer Bonding,” Journal of Microelectromechanical Systems 2011, Vol. 20, No. 1, 95–103
12. Mukhiya, R., Aditi, K., Prabakar, M., Raghuramaiah, J., Jayapandian, R., Gopal, V.K., Khanna, Shekhar, C.: Fabrication of Capacitive Micromachined Ultrasonic Transducer Array with isolation trenches using anodic wafer bonding. IEEE Sens. J. **15**(19), 5177–5184 (September 2015)
13. Gill, G.S., Kumar, S., Mukhiya, R., Khanna, V.K.: “The FEM-based Study of CMUT Cell for Vacuum-Sealed and Unsealed Cavities,” 3rd International Conference on Emerging Technologies: Micro to Nano (ETMN-2017), Oct 06–07, 2017, Solapur University, Solapur, India
14. Sharma, R., Agarwal, R.: and A. Aror,"Collapse Mode Characteristics of Parallel Plate Ultrasonic [illegible] Transducers **196**(1), 52–56 (January 2016)

15. Rahman, M., Chowdhury, S.: "An Accurate Model for Pull-in Voltage of Circular Diaphragm Capacitive Micromachined Ultrasonic Transducers (CMUT)," MEMS LAB report, Department of Electrical and Computer Engineering, University of Windsor, Ontario, Canada
16. Gill, G.S., Singh, T., Prasad, M., “Study of FBAR response with variation in active area of membrane,” AIP Conference Proceedings, Vol. 1724, Issue 1, April: 2016, pp. 920040-020040-7

Figures

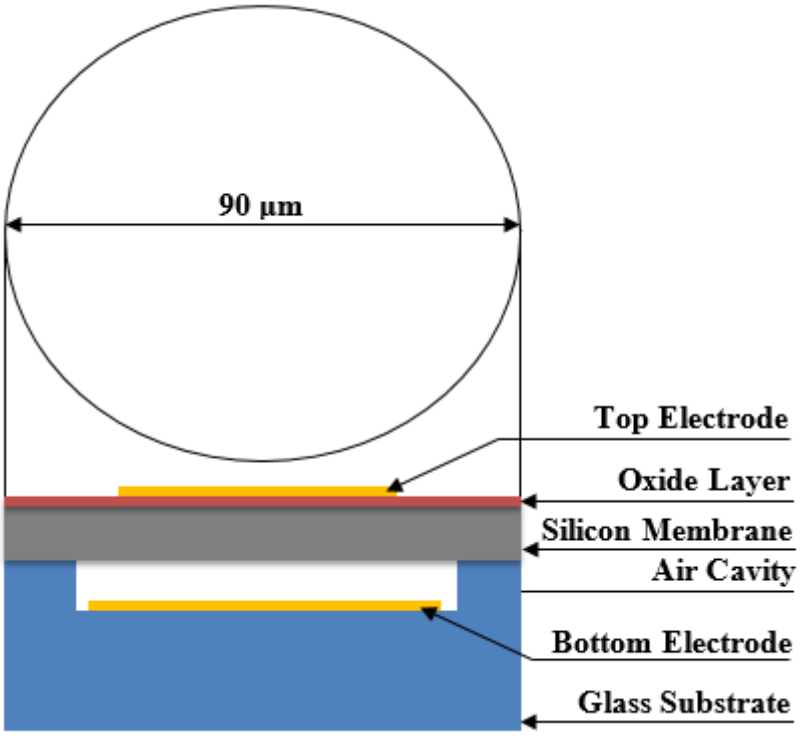

Figure 1

Cross-sectional schematic of a proposed CMUT single cell structure having diameter of 90 µm. A detailed information on layers thickness is explained in Table 1.

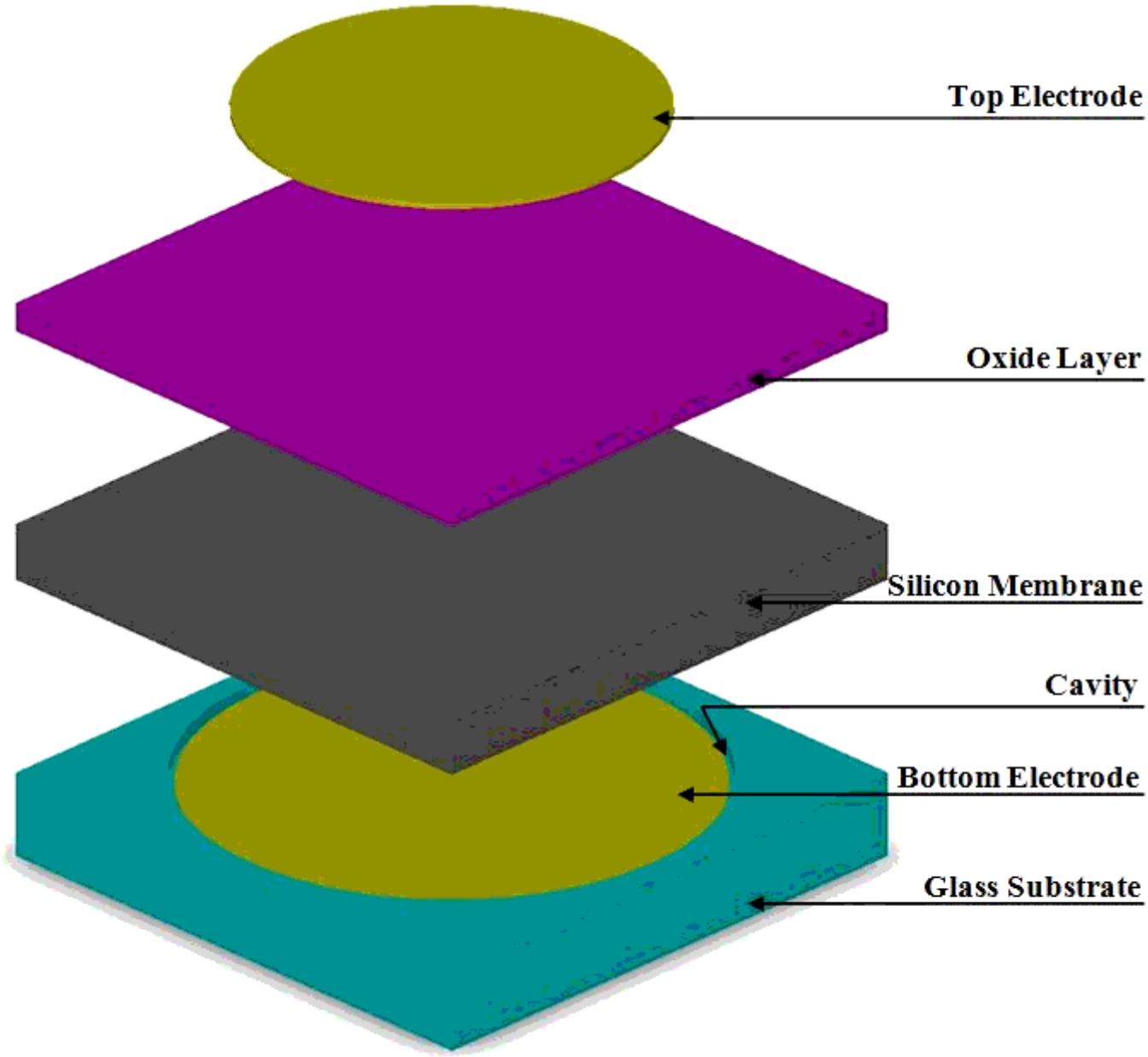

Figure 2

Process flow of circular CMUTs cell 3-D model structure using CoventorWare®.

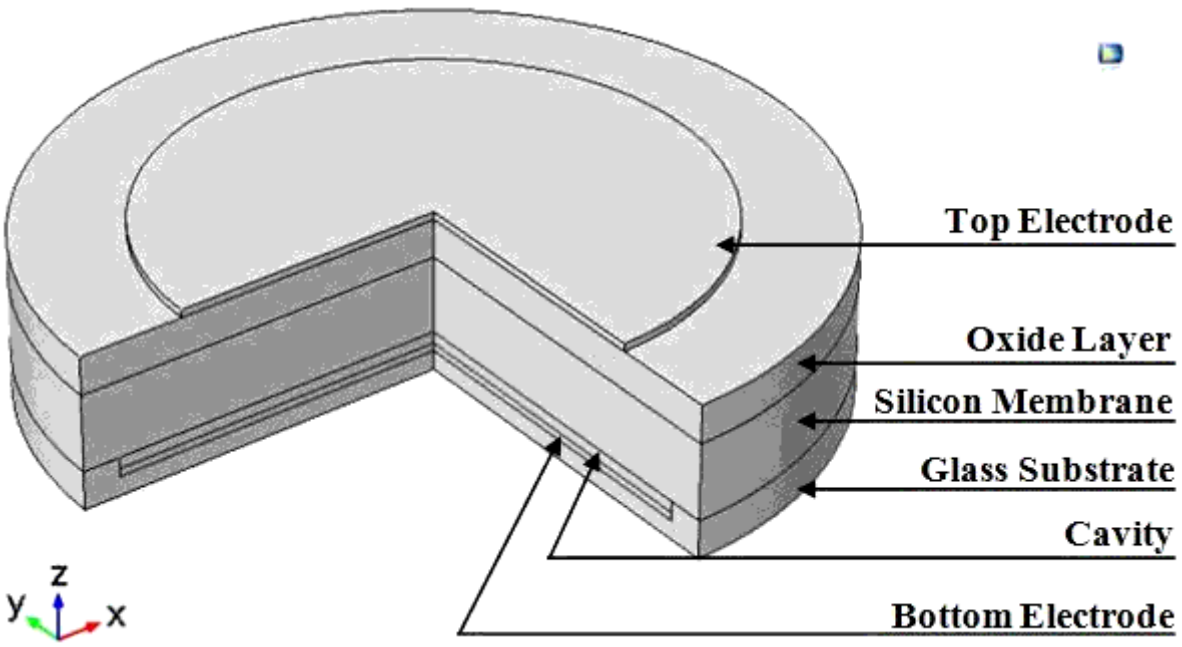

Figure 3

Cross-sectional view of CMUT cell using COMSOLTM.

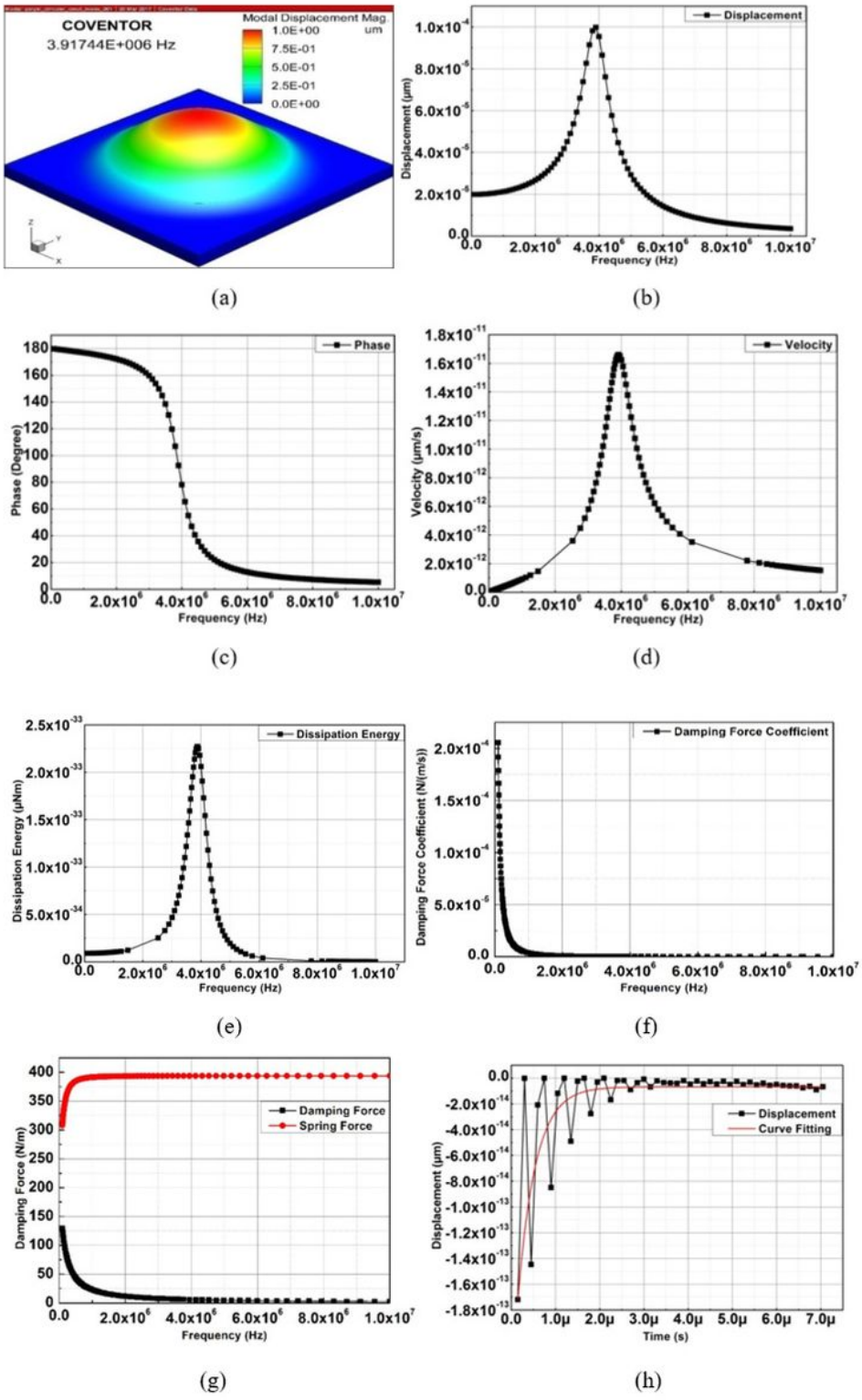

Figure 4

Various plots of circular CMUT cell using CoventorWare® tool (a) modal analysis; (b) membrane displacement at resonance frequency; (c) phase shift at resonance frequency; (d) membrane vibration velocity at resonance frequency; (e) energy dissipated in the membrane at resonance frequency; (f) damping coefficient of membrane vs. frequency (g) damping force and spring force in the membrane vs.

frequency (h) transient analysis of displacement in the membrane in order to check the settling time of membrane.

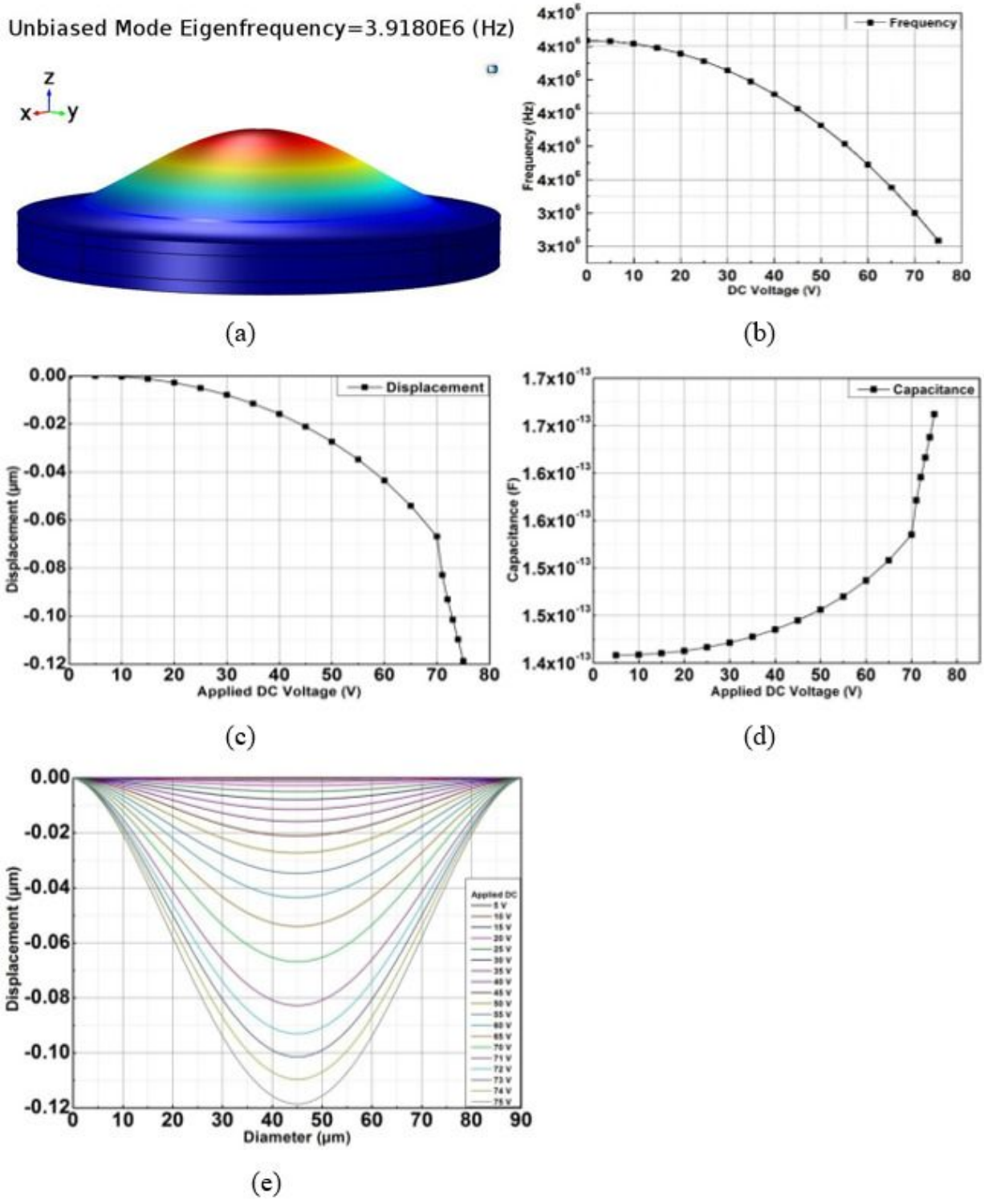

Figure 5

Various plot using COMSOLTM Tool: (a) Eigenfrequency response of CMUT cell; (b) shift in resonance frequency along with increasing DC voltage, (c) displacement in the membrane along with applied DC

voltage, (d) increase in the capacitance of CMUT cell along with applied DC voltage, (e) Membrane displacement w.r.t different applied DC voltages .

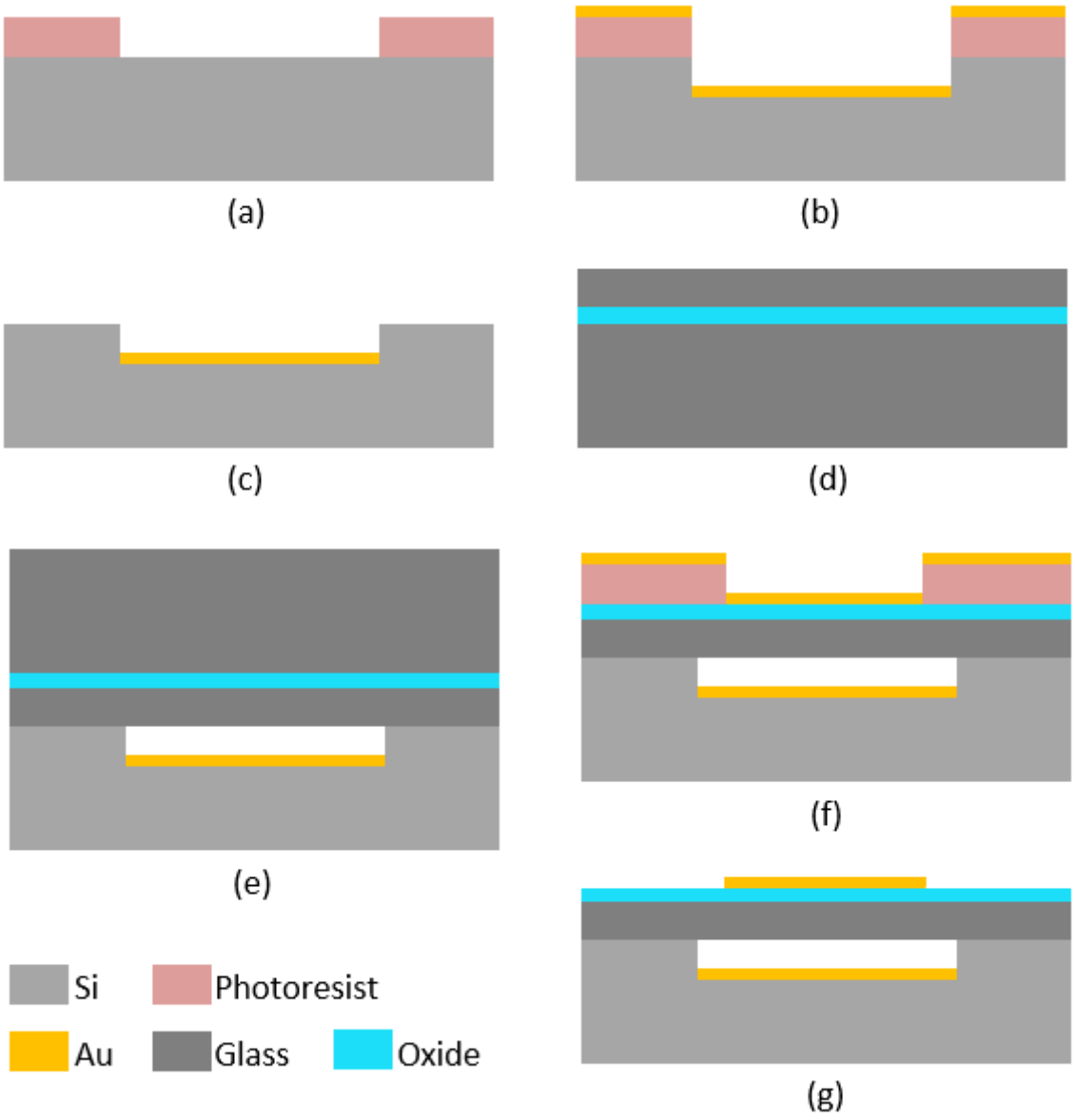

Figure 6

(a) Pyrex glass wafer coating and patterning with photoresist in order to etch the glass substrate; (b) etching of glass substrate in buffered oxide etch (BOE) solution and deposition of bottom gold electrode using sputtering technique; (c) removal of unwanted gold with the help of acetone using lift-off process; (d) Silicon-on-Insulator (SOI) wafer; (e) anodic bonding of SOI wafer on to the glass wafer and bulk handling silicon will be etched in TMAH solution; (f) spin coating and patterning of photoresist in order to deposit top gold electrode using sputtering technique; and (g) removal of unwanted gold with the help of acetone using lift-off process.